Analytical solutions to evaluate solar radiation overheating in simplified glazed rooms

Belen Moreno[a,*], Juan A. Hernández[a]

[a] *Department of Applied Mathematics, School of Aeronautical and Space Engineering, Technical University of Madrid (UPM), Plaza Cardenal Cisneros 3, 28040 Madrid, Spain*

Abstract

Calculation methods for the energy demand of buildings require the evaluation of the solar energy which is transmitted indoors through the transparent elements of the building envelope. This energy contributes to raise indoor temperature. Some of the outdoor solar beam and diffuse radiation impinging on the exterior surface of the glazings is transmitted indoors and is diffusely reflected on interior surface. After multiple diffuse reflections between walls and glazings, a proportion of this incoming radiation is absorbed by the opaque walls and the interior surface of the glazings raising the indoor temperature.

The objective of this study is to present analytical solutions for a very simple room with a glazing subjected to solar radiation with a normal angle of incidence. Namely, this study yields analytical expressions for: *(i)* the effective absorptance, *(ii)* the back absorptance of the glazing subjected to indoor diffuse irradiance and *(iii)* the indoor temperature. The effective absorptance of the room is compared with that obtained in Cucumo et al. (1995) and advanced numerical simulations are carried out by means of IDA ICE (EQUA, 2017) to validate the analytical expression for the indoor temperature.

Keywords: interior solar energy distribution; overheating; equivalent absorption; indoor temperature

Highlights

- A mathematical model is presented for a room with a glazing subjected to normal incidence radiation
- Analytical results for the indoor temperature are discussed
- Validation is carried out by means of a full numerical simulation

*Corresponding author
Email addresses: belen.moreno@upm.es (Belen Moreno), juanantonio.hernandez@upm.es (Juan A. Hernández)

List of symbols

Nomenclature	
A_{id}, A'_{id}	Front and back diffuse absorptance of glass pane i
A_I, A_{Id}	Beam and diffuse secondary internal heat transfer factor
E_b, E_d	Beam and diffuse source terms for the radiosity equations, Wm^{-2}
e_i	absorbed heat flux in surface i or glass pane i, Wm^{-2}
F_{ij}	View factor from surface i to surface j
g	Solar heat gain coefficient
G_i	Irradiance on surface i, Wm^{-2}
h_e	Exterior heat transfer coefficient, $\mathrm{Wm}^{-2}\mathrm{K}$
h_g	Heat transfer coefficient of the air chamber, $\mathrm{Wm}^{-2}\mathrm{K}$
h_i	Interior heat transfer coefficient, $\mathrm{Wm}^{-2}\mathrm{K}$
I_b, I_d	Beam and diffuse radiation Wm^{-2}
J_i	Radiosity of surface i, Wm^{-2}
Q_i	solar absorbed heat flux in surface i, W
R, R'_d	Front beam reflectance and back diffuse reflectance of the glazing
S	Area of a surface, m^2
T	Temperature, K
U	Thermal transmittance of the glazing, $\mathrm{Wm}^{-2}\mathrm{K}$
U_b	Thermal transmittance of the walls, $\mathrm{Wm}^{-2}\mathrm{K}$
N	Number of enclosure surfaces
Greek	
α	Absorptance of inner surfaces
α_e	Effective absorptance of inner surfaces
α_t	Total absorptance of transmitted solar energy
ϵ_i	Far infrared hemispherical emissivity of surface i
ϵ_r	Far infrared radiative exchange factor of two parallel surfaces
γ	Polar angle of incidence
ρ	Reflectance of inner surfaces
σ	Stefan-Boltzmann constant
τ, τ_d	Beam and diffuse transmittance of the glazing

1. Introduction

During the last two decades, all international initiatives have been aimed at reducing energy consumption as well as diminishing global warming. Kyoto Protocol (2005) was replaced by the current Paris Agreement (Paris Agreement, 2016) and the EU 2020 strategy, places special emphasis on these issues. Specifically, in the European Union, Directive 2010/31/EU (2010) aims to improve the energy performance of buildings, taking into account outdoor climatic and local conditions, as well as indoor climate requirements and cost-effectiveness. Energy consumption in buildings represents, worldwide, approximately one third of the total energy consumption. This percentage varies depending on the location and the systems used, such as building enclosure, where glazing has strengthened its position as an essential construction material in low energy buildings.

Lai and Hokoi (2015) reviewed the important content of studies on opaque, transparent or semi transparent solar facades. Solar facades are designed to specifically reject or absorb and reutilizes solar heat. Huang and lei Niu (2016) reviewed numerous studies on optimization of the building envelope based on simulated performances. Energy performance, thermal comfort and visual comfort is optimized as a multi-objective building envelope target. The influence of daylight, thermal loss and solar gain may lead to an optimum design (Garnier et al., 2015).

The increased focus on intelligent building design and constant technological advances in glass products means that integrating large glazed surfaces in low energy or passive buildings has now become even more achievable. Technological innovation such as the use of double and triple glazed units with inert gas filling and invisible low-emissivity and solar-control coatings have significantly improved the insulation properties of windows and facades, as well as new methods of modulating solar heat and light transmission, (Hee et al., 2015). Such glazing products allow natural daylight into buildings and can maximize or limit solar heat gains, depending on the desired thermal objectives and energy balance. Nowadays, architects and building engineers believe that energy efficiency has turned into one of the most determining aspects for the election of the constructive typology. The solar g factor and the thermal transmittance, U-value (EN 410, 2011), emerge as the key parameters that enable two possible energy scenarios: *(i)* energy harvesting, using windows, walls, and floors to collect, store, and distribute solar energy in the form of heat in winter and *(ii)* energy rejection of solar heat in summer, through the glass enclosure.

Improving the energy and daylighting performance of building envelope is essential issue for achieving building energy efficiency. Kim and Kim (2010a) discussed healthy residential environment as an architectural field of light. Kim and Kim (2010b) reviewed daylighting systems for capturing natural light when overcrowded urbanization does not allow to optimize building orientation and window sizes. Berardi and Wang (2014) considered daylighting in an atrium-type high performance house analyzing the visual comfort inside the house due to large areas of glazed openings. In Kazanasmaz et al. (2016), the performance of a window in terms of spatial daylight autonomy is optimized by its geometry and optical properties. In office environments, users prefer windows mostly for the attributes of daylight, sunlight and natural ventilation (Dogrusoy and Tureyen, 2007). Thermotropic materials which change their light transmission

behavior reversely have a great potential in achieving an excellent comprehensive performance between solar gain and daylighting (Yao and Zhu, 2012).

To address the energy efficiency requirement, standards such as Passivhaus has been adopted by housing sectors (Sameni et al., 2015). When adopting Passivhauss standard the thermal envelope becomes highly insulated and maximizes passive solar heat gains presenting a risk of overheating (Fletcher et al., 2017). Besides, fully–glazed facades increases overheating phenomena (Ulpiani et al., 2017). There is a growing interest in understanding overheating inside buildings and associated health risks (Baniassadi and Sailor, 2018). Possible trades–off and synergies between energy efficiency strategies and resiliency to heat in residential buildings have been studied in Jenkins et al. (2009). Poorly ventilated dwellings are vulnerable to overheating particularly if their windows are not well protected against direct solar radiation (Hamdy et al., 2017). In modern office buildings thermally–insulated envelopes enhance overheating even in cold climates (Aste et al., 2018). This negative impact of solar gains on the yearly energy balance limits the amount of glazing or recommends using external solar shading devices.

Different models have been used for the calculation of solar energy distribution with different geometries and different absorbing properties, as well as the evaluation of the distribution of the illumination and the NIR. Wall (1997) compared four such approaches for solar radiation distribution in a room and concluded that a geometrical description of the enclosed space is important and transmission through windows, reflection and absorption must be accurately taken into account.

In traditional buildings, the window-wall ratio is small and it is assumed that the incoming solar radiation cannot escape through the window. This hypothesis is not suitable for buildings with glazed facades (Lu et al., 2017). Modifications to take into account this phenomena are carried out on the basis of the Radiosity Irradiation Method. Modest (1982) was one of the first to use the the Radiosity Irridiation Method (RIM) which was developed by Sparrow and Cess (1978) for determining the illumination within a room. The RIM algorithm uses view factors and solves the radiosity and irradiation of each surface.

Cucumo et al. (1995) and Wen and Smith (2002) estimated the effective solar absorptance of a room by means of a RIM model.

Gupta and Tiwari (2005) studied the energy solar distribution inside greenhouse with and without a reflecting surface on north wall.

Model predictions in Cucumo et al. (1995) were compared with an approximate theoretical equation which took into account the solar energy absorbed by the opaque walls. However, this approach did not account for the indoor diffuse energy which is absorbed by the glazing.

Oliveti et al. (2011) discussed an accurate calculation of solar heat gain through glazed surfaces. The model used the effective absorption coefficient of the indoor environment to take into account that the entering energy is in part absorbed by the surfaces of the cavity and in part is dispersed outwards, through the same glazed surfaces. Causone et al. (2010) proposed a simplified procedure to correctly calculate the magnitude of direct solar loads. Kontoleon (2015) used a novel methodology to calculate the distribution of incoming solar energy on the internal surfaces based on sunlit pattern methodology

allowing the distribution of the incoming direct solar radiation more realistically. Chatziangelidis and Bouris (2009) developed a method that distributes the total direct solar radiation among its internal surfaces. Kumar et al. (2017) worked on experimental and theoretical studies of glazing materials to reduce cooling loads within the building.

Even with precise simulation tools, the election of the correct glazing configuration remains very complicated. There are two model approaches to deal with the simulation thermal behavior: *(i)* complete models or Computational Fluid Dynamics (CFD) models and *(ii)* simplified models such as EnergyPlus (DOE, 2010) or IDA-ICE (EQUA, 2017). These last approaches are based on the evolution in time of ordinary differential equations where experimental or analytical correlations are used to deal with heat transfer mechanism of air in rooms or chambers.

Aguilar et al. (2017) simulated the thermal performance of a room with a complete CFD model with turbulence. Xamán et al. (2016) used a finite volume method for thermal evaluation of a room with a double glazing window evaluating complete configurations of different glazing with or without a solar control film. Konroyd-Bolden and Liao (2015) used a three dimensional finite element method to study the thermal behaviour of a window. Kontoleon (2012) developed a thermal network method with distribution of internal solar radiation on different facade orientations to select the glazing to reduce building energy consumption. Optimizations of building aspect ratio and south window size (Inanici and Demirbilek, 2000) as well as design decisions based on building simulation (Augenbroe, 2002) are increasingly relevant.

A parametric study can be carried out by performing a large number of numerical simulations generating a large dataset from which conclusions are difficult to be obtained. It is therefore of great importance to be able to help architects and building engineers in the design of glazed enclosures and to correctly evaluate the consequences of using this type of solar-passive system, in terms of comfort and energy savings (Mottard and Fissore, 2007). Besides, when using EnergyPlus or IDA-ICE windows can be simulated involving approximations based on the g factor and the U-value which may lead to errors in some situations (Lyons et al., 2010). Energy Plus contains two different models to simulate windows: *(i)* the complete model, which takes into account the different layers of the glazing and *(ii)* the simplified model in which the glazing is defined by two parameters: g factor and U - value. If the first model is used, the thermal performance of the glazing is obtained by considering the different absorptions of the layers. When the simplified model is used, it is not possible to determine the amount of solar energy that is absorbed inside. Therefore, the calculated solar heat gain can be misled. Different glazings with different thermal performances may have the same g factor and U - value, misleading the thermal performance when using the simplified model.

Thermal simulation by means of complete or simplified models for normal buildings are able to perform very realistic situations. However, they do not allow to predesign or preselect a specific glass configuration for highly-glazed spaces. This is crucial for highly-glazed spaces because a considerable part of the transmitted energy can leave the room through the glazing if it is not absorbed indoors. Wall (1995, 1997) demonstrated that the percentage of the radiation retained in a sunspace, where much of the surfaces are glazed, can vary from 30% to 85%. Such spaces may improve the appearance of the building

and reduce the heating requirements of a house (Ferrante, 2000). However, an improper design may raise the energy consumption of the building or lead to frequent overheating and high temperatures that are uncomfortable (Bastien and Athienitis, 2000).

The objective of this study is to elucidate the multiple reflexion mechanism of solar radiation among the room interior surfaces in order to determine the amount of transmitted solar energy which is absorbed in all the interior surfaces of the room: walls and glazing. Hence, to achieve this goal it is essential: *(i)* to identify the main physical mechanisms and the importance of the indoor temperature of spectral and thermal parameters, *(ii)* to obtain a simple analytical expression for the indoor temperature to pre-design or to select the correct glazing configuration.

2. Spectral indoor problem

The solar radiation illuminates a glazed room giving rise to a difficult spectral problem which is called the solar indoor distribution. The sun impinges on the glazing and some part of the radiation is transmitted indoors. When light strikes some interior surface, it is diffusely reflected. Generally, interior surfaces are diffuse reflectors or emitters considered as Lambert surfaces (Baehr and Stephan, 2006).

The emissivity ϵ_i is the only material function of a gray Lambert radiator. If the radiation emitted from a surface is diffusely distributed, its emissivity is independent of the direction of emission. Hence, its hemispherical spectral absorptivity agrees with its hemispherical spectral emissivity (Baehr and Stephan, 2006). However, most surfaces behave differently in the absorption of solar radiation than in the absorption of long wave radiation coming from surface emitters or sources. The gray lambert radiator can not be applied to the absorption of solar radiation. The absorptivity of short wave solar radiation deviate vastly from the emissivity of long wave radiations (Baehr and Stephan, 2006).

In this section, a simple model of the Radiosity Irradiation Method (RIM) is presented (Sparrow and Cess, 1978). The room is divided into N different surfaces. Fig. 1, shows a generic surface S_i. The radiosity J_i is defined as the outgoing radiant flux of surface S_i per unit area (Sparrow and Cess (1978)). The view factor F_{ji} is the proportion of radiation which leaves surface S_j, that strikes surface S_i (Baehr and Stephan, 2006). The incoming radiant flux per unit area received by surface S_i and produced by the rest of surfaces S_j is called the irradiance G_i and it has the following expression:

$$G_i = \sum_{j=1}^{N} F_{ji}\ J_j\ \frac{S_j}{S_i}, \quad i = 1, \ldots, N. \tag{1}$$

The energy balance for S_i states that the outgoing radiant flux J_i is equal to the emitted radiant flux E_i plus the reflected incoming radiant flux G_i:

$$J_i\ S_i = E_i\ S_i + \rho_i\ G_i\ S_i, \quad i = 1, \ldots, N, \tag{2}$$

where, ρ_i is the reflectance of the inner surfaces.

Introducing the reciprocity rule $F_{ji}S_j = F_{ij}S_i$ (Baehr and Stephan, 2006) in Eq. (2), it simplifies to:

$$J_i = E_i + \rho_i \sum_{j=1}^{N} F_{ij} J_j, \quad i = 1, \ldots, N. \tag{3}$$

Eq. (3) is valid for every wavelength. Since short wavelengths coming from the sun are much smaller than long wavelengths emitted by normal bodies (Baehr and Stephan, 2006), a separate analysis can be made for these two wavelengths.

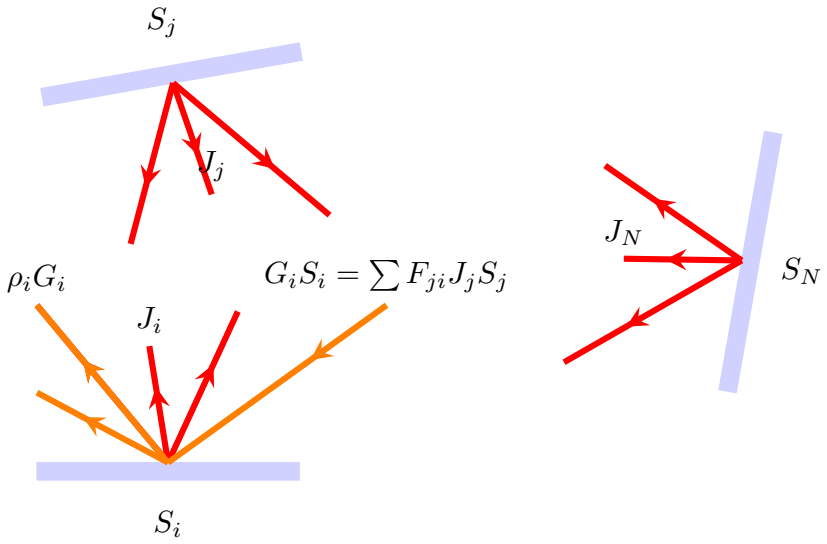

Figure 1: Outgoing radiant flux J_i or radiosity (red), contributions of other surfaces through the view factor F_{ji} to the incoming radiant flux G_i or irradiance (orange) and reflections of irradiance (orange).

2.1. Long wave spectral problem

The thermal radiation emitted from a surface is long wavelength radiation, fundamentally Far Infrared Radiation (FIR). It ranges from approximately 2500 nm to 12000 nm. Therefore, the general RIM Eqs. (3) can be integrated between the limits of 2500 nm and 12000 nm to obtain the far infrared RIM equations of the different interior surfaces of the room. If each surface is grey for the far infrared range of the spectrum, its reflectivity is independent of the wavelength in this range. Hence, its FIR hemispherical total reflectvity agrees with its hemispherical spectral reflectivity. Defining the mean values in this range as:

$$J_i = \epsilon_i \, \sigma \, T_i^4 + (1 - \epsilon_i) \sum_{j=1}^{N} F_{ij} J_j, \quad i = 1, \ldots, N, \tag{4}$$

where, σ is the Stefan-Boltzmann constant, ϵ_i is the far infrared hemispherical emissivity of surface i , $\epsilon_i \, \sigma \, T_i^4$, is the emitted radiant flux E_i Eq. (3) and T_i is the temperature of S_i. It is important to note that solar radiation does not appear in this range of wavelengths. Furthermore, the long wavelength absorptance is equal to the emissivity ϵ_i.

Once the long wavelength radiosities are known, the long wavelength heat flux e_i which is absorbed by every surface S_i can be calculated by the following expression:

$$e_i = \epsilon_i \; G_i - \epsilon_i \; \sigma \; T_i^4, \quad i = 1, \ldots, N, \tag{5}$$

where the first term represents the absorbed irradiance and the second term is the thermal radiation emitted by the surface S_i. Using Eq. (4), the above expression yields:

$$e_i = \; G_i - J_i, \quad i = 1, \ldots, N. \tag{6}$$

The absorbed heat flux or the net heat input equals irradiance minus radiosity.

2.2. Short wave spectral problem

The sun emits short wavelength radiation, fundamentally visible and Near Infrared Radiation (NIR). Ranging from approximately 350 nm to 2500 nm. When the general RIM Eqs. (3), are integrated between these wavelengths, the radiosities J_i are given by the following equation:

$$J_i = E_{di} + \rho_i \; E_{bi} \; cos\gamma_i + \rho_i \sum_{j=1}^{N} F_{ij} J_j, \quad i = 1, \ldots, N. \tag{7}$$

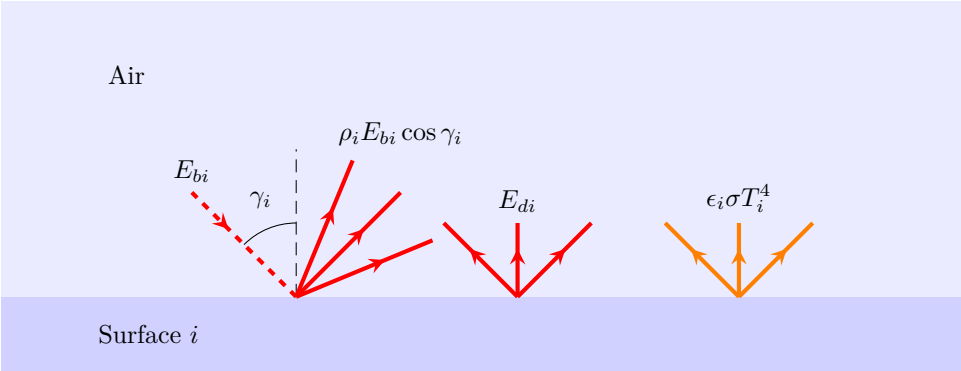

Figure 2: Different source terms for the visible and near infrared (red) and source terms for far infrared (orange).

In this range of wavelengths, diffuse solar radiation E_{di} and projected beam solar radiation E_{bi} are the sources which give rise to irradiance in these wavelengths. Note that there is no thermal radiation in this range of wavelengths. The different sources terms are shown graphically in Fig. 2. In this figure, the impinging direct beam radiation E_{bi}, which has an angle of incidence γ_i, is reflected diffusely originating the diffuse source term $\rho_i \; E_{bi} \cos\gamma_i$. Moreover, if the surface is transparent or translucent, it can be illuminated by an external diffuse source giving rise to the source term E_{di}.

Once the visible and near infrared radiosities are calculated from Eq. (7), the visible and near infrared heat fluxes absorbed by each surfaces S_i can be calculated. The heat flux absorbed by surface S_i is the sum of the absorbed irradiance G_i and the solar beam radiation absorbed by the surface S_i:

$$e_i = \alpha_i \left(G_i + E_{bi} \; cos\gamma_i \right), \quad i = 1, \ldots, N, \tag{8}$$

where α_i is the absorptance of inner surfaces.

In summary, the solar energy distribution in FIR is governed by Eq. (4) whereas, Eq. (7) represents the solar energy distribution in NIR. Eq. (4) contains one source term: the temperature at which each surface emits energy. The multiple reflections mechanism originates the different radiosities in the FIR regime. Besides, Eq. (7) allows to obtain the radiosities in NIR and in visible spectra, through two source terms: *(i)* the diffuse solar radiation originated by the external diffuse solar radiation (E_{di}) and *(ii)* the first reflection that occurs inside the room from the beam radiation (E_{bi}).

3. Radiosity and irradiance solutions for a room defined by two surfaces

The analysis of a conventional room with various glazings, doors and walls is very complicated and requires numerical simulations to obtain accurate results.

In this section, we particularize the energy balance of radiant fluxes (Eqs. (3)) for a room composed of two surfaces. The surface of the glazing is denoted by S_1 and the rest of the interior surface is denoted by S_2. While the glazing is considered a flat surface, the surface of the interior are the walls, floor and ceiling as it is shown in Fig. 3. The solar beam radiation is considered normal to the glazing.

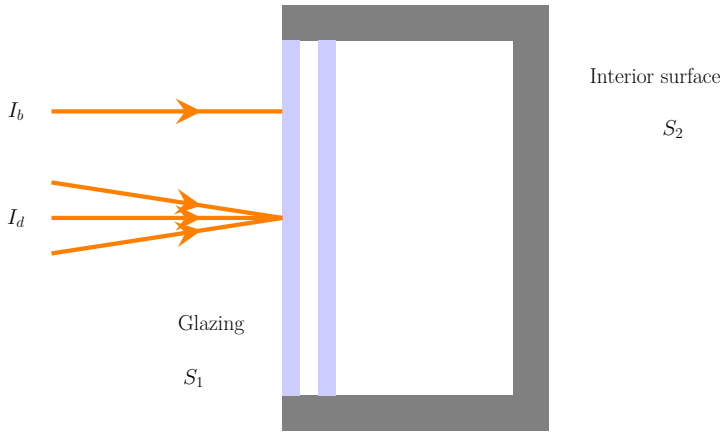

Figure 3: Simplified room composed by two surfaces: glazing S_1 and interior surface S_2. Solar irradiance is composed of beam I_b and diffuse I_d radiation.

Once the interior surface have been discretized properly, the solar energy distribution of a real problem relies on the detailed solar energy distribution given by Eq. (3) . However, it is very difficult to cover all different thermal and spectral configurations to discover the relevant parameters. Therefore, an effort to obtain an analytical solution for a simplified room will allow to grasp the physical mechanisms of the solar energy distribution.

When only two surfaces S_1 and S_2 are considered, the system of Eqs. (3) is:

$$\begin{bmatrix} 1-\rho_1\ F_{11} & -\rho_1\ F_{12} \\ -\rho_2\ F_{21} & 1-\rho_2\ F_{22} \end{bmatrix} \begin{bmatrix} J_1 \\ J_2 \end{bmatrix} = \begin{bmatrix} E_1 \\ E_2 \end{bmatrix}. \tag{9}$$

These equations are solved to give rise to the following radiosities:

$$J_1 = \frac{(1-\rho_2\ F_{22})\ E_1 + \rho_1\ F_{12}\ E_2}{(1-\rho_1\ F_{11})(1-\rho_2\ F_{22}) - \rho_1\ \rho_2\ F_{12}\ F_{21}}, \tag{10}$$

and

$$J_2 = \frac{(1-\rho_1\ F_{11})E_2 + \rho_2\ F_{21}\ E_1}{(1-\rho_1\ F_{11})(1-\rho_2\ F_{22}) - \rho_1\ \rho_2\ F_{12}\ F_{21}}. \tag{11}$$

Once the radiosities are obtained, the irradiance of each surface can be obtained to give:

$$G_1 = F_{11}\ J_1 + F_{12}\ J_2, \qquad G_2 = F_{21}\ J_1 + F_{22}\ J_2. \tag{12}$$

4. Analytical solution for radiosities of a room with a small ground surface

In this section, the above model is simplified in order to neglect reflections of walls. Therefore, floor or ground surface are considered very small compared to the glazing surface S_1. This hypothesis is equivalent to saying that the interior surface $S_2 \approx S_1$. Since the glazing surface S_1 is flat, the view factor $F_{11} = 0$ and, consequently, $F_{22} = 0$. Since the sum of the rows of the view factor matrix is equal to one (Baehr and Stephan, 2006), then $F_{12} = 1$ and $F_{21} = 1$.

4.1. Long wave solution

As it has been discussed in section 2, the distribution of far infrared and near infrared wavelengths should be calculated separately. When dealing with this long wave regime, the reflectance of each surface is $\rho_1 = 1 - \epsilon_1$ and $\rho_2 = 1 - \epsilon_2$ where ϵ_1 and ϵ_2 are the emissivities for each surface. Since the glazing is opaque to long wavelengths, the only sources inside the room are due to the emitting properties of the surface $E_1 = \epsilon_1\sigma\ T_1^4$ and $E_2 = \epsilon_2\sigma\ T_2^4$. Taking these values to Eqs. (10) and (11), the following radiosities are obtained:

$$J_1 = \frac{\epsilon_1\ \epsilon_2}{\epsilon_1\ \epsilon_2 - (1-\epsilon_1)(1-\epsilon_2)}\sigma\ T_1^4, \qquad J_2 = \frac{\epsilon_1\ \epsilon_2}{\epsilon_1\ \epsilon_2 - (1-\epsilon_1)(1-\epsilon_2)}\sigma\ T_2^4. \tag{13}$$

From Eq. (6), heat fluxes are obtained:

$$e_1 = -e_2 = \epsilon_r\sigma(T_2^4 - T_1^4), \tag{14}$$

where ϵ_r is defined by:

$$\frac{1}{\epsilon_r} = \frac{1}{\epsilon_1} + \frac{1}{\epsilon_2} - 1. \tag{15}$$

This is the classical solution for the heat flux interchange between two planes at different temperatures (Baehr and Stephan, 2006).

4.2. Short wave solution or solar energy distribution

For the visible and near infrared regime the situation is different. The glazing is transparent to short wavelengths coming from the sun and, consequently, different source terms are present. First, the transmitted solar beam radiation τI_b is considered. This beam radiation impinges on S_2. Some part of the radiation is absorbed $\alpha\tau I_b$, and the rest is reflected diffusely to create a source term $E_2 = \rho\tau I_b$ and later give rise to inner radiosities. Moreover, the diffuse component of the transmitted solar radiation creates the source term in the glazing $E_1 = \tau_d I_d$. The diffuse back reflectance $\rho_1 = R'_d$ of the glazing (Romero and Hernández, 2017) together with the reflectance of inner walls $\rho_2 = \rho$ allow to determine the inner radiosities.

When Eqs. (10) and (11) are particularized for these values, the radiosities of the interior surface of the glazing and the interior wall are:

$$J_1 = \frac{\tau_d\ I_d + R'_d\ \rho\ \tau\ I_b}{1 - R'_d\ \rho}, \tag{16}$$

and

$$J_2 = \frac{\rho\ (\tau_d\ I_d + \tau\ I_b)}{1 - R'_d\ \rho}. \tag{17}$$

Since $F_{11} = F_{22} = 0$ and $F_{12} = F_{21} = 1$, the irradiance of the interior surface of the glazing is equal to the radiosity of the insulated wall ($G_1 = J_2$) and the irradiance of the insulated wall is equal to the radiosity of interior surface of the glazing ($G_2 = J_1$). The interior wall absorbs the following heat flux per square meters given by Eq. (8):

$$e_2 = \alpha\,(G_2 + \tau I_b) = \frac{\alpha\,(\tau_d\ I_d + \tau I_b)}{1 - R'_d\ \rho}, \tag{18}$$

where $\alpha = 1 - \rho$ is the absorptance of the inner wall. In Eq. (18), $\tau_d I_d + \tau I_b$ represents the indoor transmitted solar energy. The proportion of this energy which is absorbed by the wall is:

$$\alpha_e = \frac{\alpha}{1 - R'_d\ \rho}, \tag{19}$$

which is called the effective solar absorptance of the inner wall. It is important to note that this absorptance α_e is larger than the absorptance of an isolated wall α. This is due to the mechanism of multiple reflections between the glazing and the wall.

5. Analytical solution for radiosities of a rectangular room

In order to simplify the analytical solution, in the previous section it was assumed that the floor surface was much smaller than the glazing surface. To analyze the effect of multiple reflections in a more realistic situation, no limitations of inner surfaces are imposed in this section. The solar beam radiation is considered with a normal angle of incidence as in the previous case. Fig. 3 is also valid to represent this configuration. As in the previous case, the glazing surface S_1 is flat and, consequently, the view factor $F_{11} = 0$. On the contrary, the inner surface of the room is not flat and $F_{22} \neq 0$. To determine the view

factors of these two surfaces, it is used: *(i)* the reciprocity rule (Baehr and Stephan, 2006) and *(ii)* the fact that the sum of the columns of a specific row of the view factor matrix is equal to one.

$$F_{11} + F_{12} = 1, \tag{20}$$

$$F_{21} + F_{22} = 1, \tag{21}$$

$$F_{21}\ S_2 = F_{12}\ S_1. \tag{22}$$

Introducing $F_{11} = 0$ in Eqs. (20)–(22), we obtain:

$$F_{12} = 1, \qquad F_{21} = \frac{S_1}{S_2}, \qquad F_{22} = 1 - \frac{S_1}{S_2}. \tag{23}$$

5.1. Long wave solution

The solutions for the radiosities are similar to those obtained in section 4.1 but in this case the ratio S_1/S_2 appears. Equations (10) and (11) together with Eq. (6) allow to obtain the heat flux e_2 per square meter which is absorbed in the inner surfaces:

$$e_1\ S_1 = -e_2\ S_2 = S_1\ \epsilon_r\ \sigma(T_2^4 - T_1^4), \tag{24}$$

where ϵ_r is defined by:

$$\frac{1}{\epsilon_r} = \frac{1}{\epsilon_1} + \frac{S_1}{S_2}\left(\frac{1}{\epsilon_2} - 1\right). \tag{25}$$

This solution for the heat flux interchange between two planes at different temperatures can be found in Baehr and Stephan (2006).

5.2. Short wave solution or solar energy distribution

As in the previous case, it is assumed that the outdoor solar beam radiation is normal to the glazing. Again, two source terms of solar radiation are considered: *(i)* the transmitted diffuse radiation by the glazing $E_1 = \tau_d I_d$ and *(ii)* the reflexion of the solar beam radiation entering through the glazing $E_2 = \rho\ \tau I_b\ S_1/S_2$. Note that since E_2 is the source term in surface S_2 per square meter, the factor S_1/S_2 takes into account the entrance of the solar beam radiation through the surface S_1.

Using the view factors given by Eqs. (23) and substituting $\rho_1 = R'_d$ and $\rho_2 = \rho$ in Eqs. (12), the irradiances over surface S_1 and S_2 are obtained:

$$G_1 = \frac{\rho\ F_{21}(\tau_d I_d + \tau I_b)}{1 - R'_d\ \rho\ F_{21} - \rho\ F_{22}}, \tag{26}$$

and

$$G_2 = \frac{F_{21}(\tau_d I_d + \rho\ \tau I_b(F_{21} R'_d + F_{22}))}{1 - \ \rho\ F_{21} - \rho\ F_{22}}. \tag{27}$$

Once the irradiances G_1 and G_2 are known, Eq. (8) is used to calculate the heat flux absorbed by surface S_2 per square meter

$$e_2 = \alpha_e\,(\tau_d I_d + \tau I_b)\,\frac{S_1}{S_2}. \tag{28}$$

In this expression α_e is the effective absorptance of surface S_2 and it is given by the following expression:

$$\alpha_e = \frac{\alpha}{1 - R'_d\ \rho\ \dfrac{S_1}{S_2} - \rho\left(1 - \dfrac{S_1}{S_2}\right)}, \tag{29}$$

which takes into account the proportion of the incoming solar energy $(\tau_d I_d + \tau I_b)$ S_1 absorbed by surface S_2. Note Eq. (12) reduce to that obtained in section 4.2 when $S_1 = S_2$.

Fig. 4 shows a schematic drawing of multiple reflections to understand the expression (29). In this figure successive reflections between different surfaces are shown. The multiple reflections can be grouped in two sets: *(i)* direct reflections between glazing and parallel surfaces and *(ii)* indirect reflections between glazing, parallel surface and perpendicular surfaces. These two groups of successive reflections are shown in Fig. 4. Every time the diffuse radiation is reflected, some part of the incoming energy is absorbed. This absorption is represented in Fig.4 in red. If the series of infinitesimal absorptions is summed up, Eq. (29) is obtained.

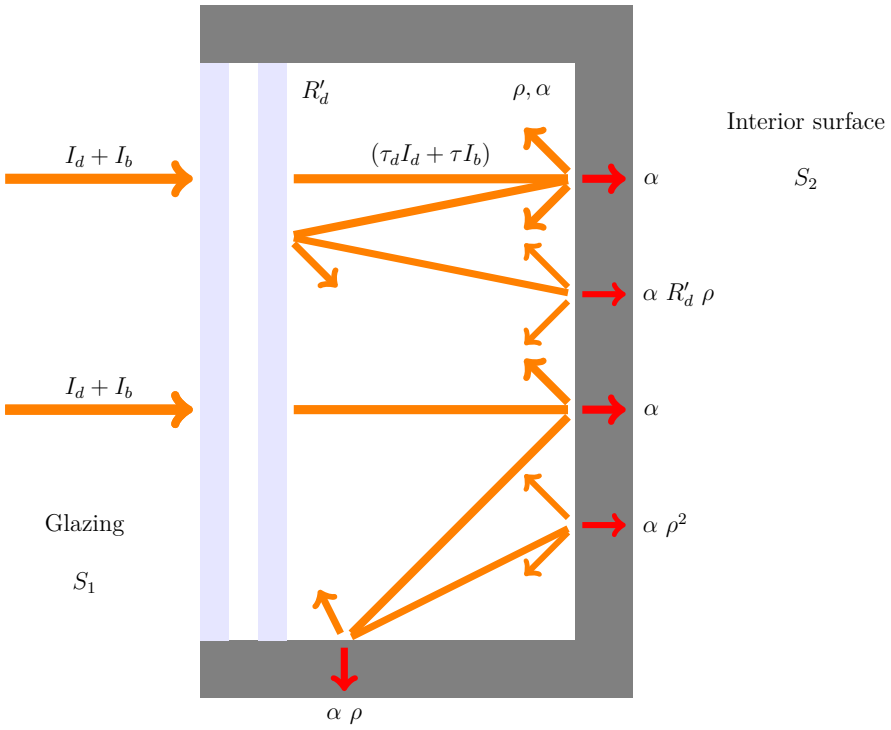

Figure 4: Multiple diffuse reflections. Direct reflections between glazing and parallel surface. Indirect reflections between glazing, parallel surface and perpendicular surfaces. Reflections in orange and heat flux absorptance in red.

Fig. 5 shows the difference between effective absorptance in a room with a small floor surface given by Eq. (19) and the effective absorptance of a generic rectangular room given by Eq. (29). The total absorbed heat flux in the interior surface $Q_2 = e_2 S_2$ is from Eq. (28):

$$Q_2 = \alpha_e\,(\tau_d I_d + \tau I_b)\,S_1. \tag{30}$$

For a given glazing surface S_1, the amount of the absorbed energy Q_2 depends on the ratio S_1/S_2 through α_e. There are two limit cases: *(i)* the area of the glazing is much smaller than the area of the insulated

walls ($S_1 \ll S_2$) and *(ii)* the area of the glazing is the same as the area of the interior surface. The absorbed energy Q_2 reaches a maximum value when the interior surface S_2 is much larger than the glazing surface S_1 as it is represented in Fig.4. On the contrary, when $S_2 = S_1$, some part of the energy entering through the glazing escapes to the exterior not being absorbed by interior surfaces S_2 (Wall, 1995), (Wall, 1997).

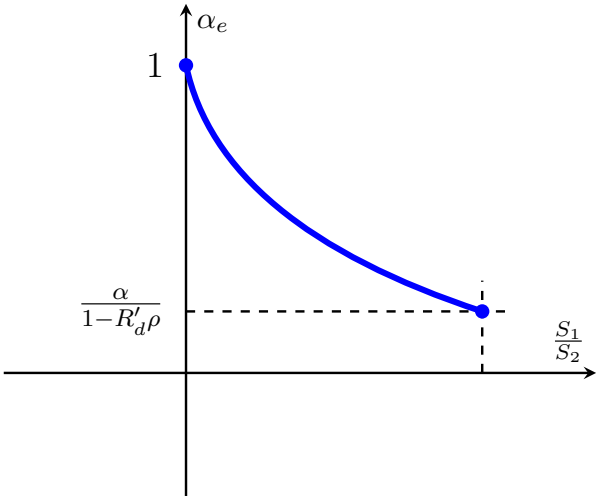

Figure 5: Variation of effective absorptance α_e with the ratio between the glazing surface S_1 and the wall surface S_2 for a simplified room. The back diffuse reflectance of the glazing is R'_d, the reflectance of the wall is ρ and its absorptance α.

The present result of the effective absorptance is compared with existing results given in Cucumo et al. (1995) and Duffie and Beckman (2013). Since the diffuse back irradiance impinging on the glazing is transmitted (τ'_d), reflected (R'_d) or absorbed (A'_d), then the sum of these radiant fluxes is equal to one:

$$\tau'_d + R'_d + A'_d = 1. \tag{31}$$

In order to compare the effective absorptance α_e (Eq. 29) with existing results (Cucumo et al., 1995) and using Eq. (31), α_e is rewritten in the following form:

$$\alpha_e = \frac{\alpha G_2}{\alpha G_2 + (A'_d \ + \tau'_d)\ \rho\ \dfrac{S_1}{S_2}\ G_2}. \tag{32}$$

The denominator of this expression could be interpreted as follows: the irradiance (G_2) of surface S_2 can be absorbed by the interior walls (αG_2), and reflected towards the glazing ($\rho S_1/S_2 G_2$). This reflected radiation can be absorbed by the glazing ($A'_d \rho S_g/S G_2$) or transmitted outdoors through the glazing ($\tau'_d \rho S_g/S G_2$). The approximate theoretical expression for the same configuration proposed in Cucumo et al. (1995) is:

$$\alpha_e = \frac{\alpha G_2}{\alpha G_2 + \tau'_d \ \ \rho\ \frac{S_1}{S_2}\ G_2}. \tag{33}$$

As it can be easily seen from (32) and (33), the analytical expression obtained in this study is reducible to the one obtained in Cucumo et al. (1995) if the back diffuse absorptance of the glazing is negligible. Hence, the indoor diffuse radiation impinging on the interior surface of the glazing is only transmitted outdoors or reflected indoors.

6. Analytical solution of the thermal problem of a room: indoor temperature

In this section, a simplified room composed of conventional double glazing of surface S_1 with an insulated surface S_2, is considered (Fig.6). Using the analytical solar distribution for this configuration obtained in section 5.2, the energy balance for glass panes and inner surface is presented.

In order to simplify the solution, the thermal mass of the room and the glass panes will be considered negligible (Sierra and Hernández, 2017). Furthermore, if the outdoor boundary conditions (I_b, I_d, T_e) are considered constant, the problem becomes steady. If the problem is steady and the thermal mass is negligible, the energy balance states that the absorbed solar energy e_i must be equal to the sum of left and right heat fluxes for each glass pane or wall. These right and left heat fluxes for each glass pane of wall, are given by Newton's law (Sierra and Hernández, 2017).

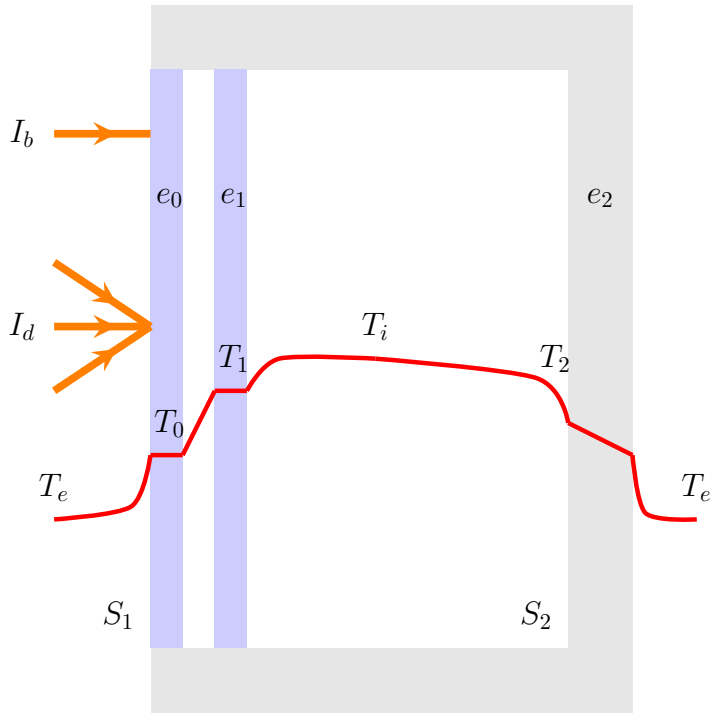

Figure 6: Thermal problem of an insulated room subjected to beam I_b and diffuse I_d solar radiation. Numbering description of solar absorbed heat fluxes (e_0, e_1, e_2), constant temperatures of glass panes (T_0, T_1) and inner surface (T_2).

To maintain the same numbering description as in section 5.2, subscript 0 has been introduced to represent the outer glass pane. For this configuration shown in Fig.6, the energy balance gives:

$$e_0 = h_e\ (T_0 - T_e) + h_g\ (T_0 - T_1), \tag{34}$$

$$e_1 = h_i\ (T_1 - T_2) + h_g\ (T_1 - T_0), \tag{35}$$

$$e_2 = U_b\ (T_2 - T_e) + h_i\ (T_2 - T_1)\frac{S_1}{S_2}, \tag{36}$$

where e_0, e_1, e_2 is the absorbed solar energy, T_0, T_1 are the glass pane temperatures, T_2 is the surface temperature of walls, h_e is the exterior heat transfer coefficient, h_i is the interior heat transfer coefficient, h_g the heat transfer of the air chamber and U_b the thermal transmittance of the walls. Equations (34)–(36) allow to determine the unknown T_0, T_1 and T_2 if the absorption energy e_0, e_1 and e_2 together with the exterior temperature T_e are known. The heat transfer coefficients h_i, h_e and h_g are given constants or can be determined as a function of surface temperatures (EN 673, 2011).

Once the spectral problem of the glazing is solved (Romero and Hernández, 2017) and the solar energy distribution is calculated (section 5.2), the energy absorbed in each glass pane or in the room walls is given by:

$$e_0 = A_0 I_b + A_{0d}\ I_d + A'_{0d}\ G_1, \tag{37}$$

$$e_1 = A_1 I_b + A_{1d}\ I_d + A'_{1d}\ G_1, \tag{38}$$

$$e_2 = \alpha_e(\tau\ I_b + \tau_d\ I_d)\frac{S_1}{S_2}, \tag{39}$$

where A_0 and A_1 denote the front beam absorptance of the glass panes, A_{0d} and A_{1d} the front diffuse absorptance of the glass panes, A'_{0d} and A'_{1d} the back diffuse absorptance of the glass panes and τ, τ_d the beam and diffuse transmittance of the glazing. In these expressions G_1 is given by Eq. (26) and α_e by Eq. (29).

Since the thermal mass of the indoor air is negligible, the energy balance for the air states that the air temperature or the inner temperature T_i is weighted between T_1 and T_2 depending on the surfaces S_1 and S_2,

$$T_i = \frac{T_1\ S_1 + T_2\ S_2}{S_1 + S_2}. \tag{40}$$

A solution of Eq. (34)–(36), using expressions (37)–(39), is substituted in Eq. (40) to give:

$$T_i = T_e + \left(\frac{1+\beta_1}{1+\delta}\right)\left[\frac{e_0}{h_e} + \left(\frac{1}{h_g} + \frac{1}{h_e}\right)e_1\right] + \left(\frac{1-\beta_2}{1+\delta}\right)\left[\frac{e_2 S_2}{U S_1}\right], \tag{41}$$

with

$$\beta_1 = \frac{U_b S_2}{(S_1+S_2)h_i}, \quad \beta_2 = \frac{U S_1}{(S_1+S_2)h_i}, \quad \delta = \frac{U_b S_2}{U S_1}, \quad \frac{1}{U} = \frac{1}{h_e} + \frac{1}{h_g} + \frac{1}{h_i}. \tag{42}$$

Since the thermal transmittance of the wall U_b and the thermal transmittance of the glazing U are usually much smaller than h_i, then $\beta_1 \ll 1$ and $\beta_2 \ll 1$. With these assumptions, the expression for T_i given by Eq. (40) simplifies to yield:

$$T_i = T_e + \frac{S_1}{U S_1 + U_b S_2}\left[A_I I_b + A_{Id} I_d + (\tau\ I_b + \tau_d\ I_d)\ \alpha_t\right], \tag{43}$$

where A_I, A_{Id} are beam and diffuse secondary internal heat transfer factors (Sierra and Hernández, 2017) given by the following expressions:

$$A_I = U\left[A_0\left(\frac{1}{h_e}\right) + A_1\left(\frac{1}{h_e} + \frac{1}{h_g}\right)\right], \tag{44}$$

$$A_{Id} = U\left[A_{0d}\left(\frac{1}{h_e}\right) + A_{1d}\left(\frac{1}{h_e} + \frac{1}{h_g}\right)\right]. \tag{45}$$

The irradiance which is absorbed by the room and by the glazing, increasing the indoor temperature, is measured by α_t which has the following expression:

$$\alpha_t = \alpha_e + \frac{\rho\ A'_{1d}\dfrac{S_1}{S_2}}{1 - R'_d\ \rho\ \dfrac{S_1}{S_2} - \rho\left(1 - \dfrac{S_1}{S_2}\right)}. \tag{46}$$

This coefficient α_t is the proportion of the transmitted energy $\tau\ I_b + \tau_d\ I_d$ which is absorbed by the room and by the glazing to increase the indoor temperature.

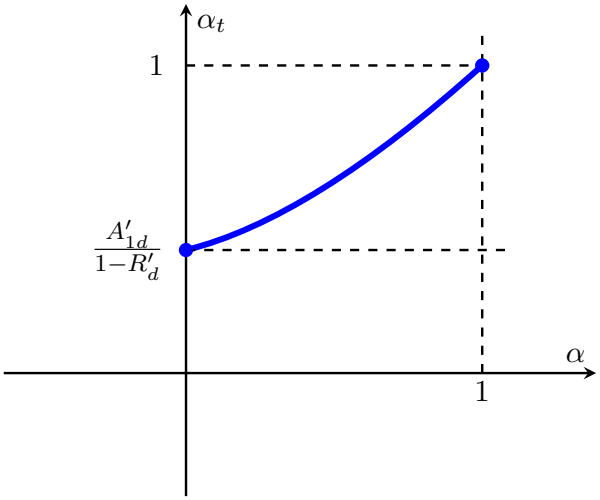

Figure 7: Variation of total absorptance α_t of wall surface S_2 as a function of the wall absorptance α. The back diffuse absorptance of the inner glass pane is A'_{1d} and the back diffuse reflectance is R'_d.

Fig. 7 shows α_t for different values of the surface absoprtance α. If the inner wall is considered a black body ($\alpha = 1$), the transmitted energy is totally absorbed. On the contrary, if a white body is considered ($\alpha = 0$), a proportion of this transmitted energy is absorbed $\alpha_t = A'_{1d}/(1 - R'_d)$ contributing to the rise of the indoor temperature. In this case, the energy is absorbed in the second glass pane and later it is radiated indoors. Depending on the back diffuse absorptance of the inner glass pane A'_{1d}, the absorbed energy of the inner walls may have low dependence on its surface absorptance α.

In order to link the present study with the definition of the g factor, Eq. (43) can be rewritten in the following way:

$$T_i = T_e + \frac{S_1}{US_1 + U_bS_2}\Big[(A_I + \alpha_t\tau)\ I_b + (A_{Id} + \alpha_t\tau_d)\ I_d\Big], \tag{47}$$

which represents the beam and diffuse solar radiation that is absorbed in the room. The solar g factor of a glazing allows to determine which proportion of the incoming solar energy is transmitted indoors and it is defined EN 410 (2011) by:

$$g = A_I + \tau. \tag{48}$$

The g factor given by Eq. (48) has two terms: *(i)* A_I which represents the transmitted energy that is already absorbed in the glazing and later radiated indoors and *(ii)* τ which represents the electromagnetic

energy associated to short and long wavelengths that is transmitted indoors. Since the g factor and the U - value are defined for an isolated glazing, these parameters are insufficient to select the glazing when considering a complete room. These parameters are insufficient to gauge the absorption of the inner layer of the glazing and the interior walls.

The analytical solution (47) allows to determine the amount of the transmitted energy which is absorbed, increasing the indoor temperature. The absorbed energy is α_t given by Eq. (46) and can vary depending on the surface absorptance as it is shown in Fig.7.

The energy balance of a room states that the absorbed energy in the glazing and in the room is equal to the energy loses through the envelope. Hence, if the proportion of the incoming energy (α_t) is known, then the indoor temperature is obtained. This value α_t is greater than the effective absorption α_e and greater than the absorptance of the wall α,

$$\alpha_t > \alpha_e > \alpha. \tag{49}$$

The reason is associated to multiple reflection mechanism. When the incoming solar energy impinges on a wall the first ray is absorbed. The expression (47) allows to grasp the influence of different layers and coatings on the indoor temperature.

To increase the indoor temperature, two operations can be implemented: *(i)* increase the insulation of the walls or the glazing and *(ii)* maximize the absorbed energy by the walls and the glazing. This absorbed energy depends on A_I, τ, α_t. Since $h_e >> h_i$, the influence of the absorptance of the outermost pane A_0 is negligible and A_1 becomes significant in A_I according to Eq. (44). High values of glazing transmittance τ allows to maximize the absorbed energy. Furthermore, from Eqs. (29) and (46), α_t can be rewritten in the following way:

$$\alpha_t = \frac{\alpha + \rho \;\; A'_{1d} \; \dfrac{S_1}{S_2}}{1 - R'_d \; \rho \; \dfrac{S_1}{S_2} - \rho \left(1 - \dfrac{S_1}{S_2}\right)}, \tag{50}$$

where the main parameters that greatly influence in α_t are A'_{1d} and R'_d. The larger these parameters are, the higher the absorptance α_t.

Conversely, to decrease the indoor temperature, two operations can be implemented: *(i)* decrease the insulation of the walls or the glazing and *(ii)* minimize the absorbed energy by the walls and the glazing. The smaller the absorptance A_1, the lower the heat transfer factor A_I. This is usually obtained selecting an extraclear glass without coatings for the inner pane. For a small τ value, decreasing α_t minimizes the absorbed energy. This can be accomplished by decreasing A'_{1d} and R'_d. Since the absorptance of coatings is significant, an appropriate position in the glazing panes achieves the above strategies.

7. Numerical results and model verification

To clarify the overheating problem associated to the indoor temperature discussed in Section 6, some numerical results are analyzed. Furthermore, this section addresses the verification of the analytical

result for the indoor temperature given by expression (47). The verification process was carried out by complete simulations performed by the commercial software IDA ICE.

Two different double glazings were studied: *(a)* a solar protection double glazing and *(b)* a solar gain double glazing. The two glazings have an Argon chamber of 16 mm. and clear glass panes of 6 mm. While the solar protection glazing has a reflective coating in surface 2, the solar gain double glazing has low emissivisity coating in surface 3 (Fig.8).

The spectral properties of these two glazings were extracted from IDA ICE variables and were summarized in Table 1 for the beam, diffuse and back absorptances and Table 2 for transmittances, reflectances and emissivities of the glazing.

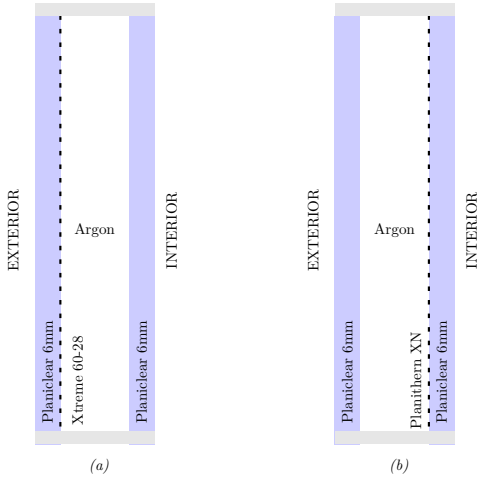

Figure 8: Double glazings for verification and comparison: *(a)* solar protection double glazing and *(b)* a solar gain double glazing

Glazing	A_0	A_1	A_{0d}	A_{1d}	A'_{0d}	A'_{1d}
Solar protection	0.303	0.020	0.306	0.021	0.153	0.118
Solar gain	0.085	0.070	0.098	0.069	0.050	0.129

Table 1: Spectral absorptances of a solar protection glazing and a solar gain glazing.

Glazing	τ	τ_d	R'_d	ϵ_0	ϵ_1
Solar protection	0.248	0.208	0.520	0.021	0.84
Solar gain	0.580	0.493	0.326	0.84	0.05

Table 2: Transmittance, reflectance and emissivities of a solar protection glazing and a solar gain glazing.

Summer and winter conditions are analyzed for the two glazing configurations. The summer test case is defined by an outdoor temperature $T_e = 35^o$C, a beam solar radiation $I_b = 200$ Wm^{-2} and a diffuse solar radiation $I_d = 0$. Winter test case is defined by an outdoor temperature $T_e = 5^o$C, beam solar radiation $I_b = 0$ and diffuse solar radiation $I_d = 75$ Wm^{-2}.

To evaluate the absorption of the transmitted solar energy into the room, different dimensions of the same geometry are evaluated. The room is considered a rectangular parallelepiped in which one facade is a glazing of surface S_1 and the rest of the surfaces are opaque walls of surface S_2.

Regarding thermal parameters, the coefficients h_i and h_e are taken from the European Standard (EN 673, 2011), being $h_i = 8$ Wm^{-2} K and $h_e = 23$ Wm^{-2} K for vertical glazings. The heat transfer coefficient h_g is calculated according to the European Standard (EN 673, 2011) to determine the radiation contribution and the convective transport mechanism associated to the argon. The thermal transmittance of the envelope $U_b = 0.3$ Wm^{-2} K represents approximately ten centimeters of insulation.

In Fig. (9) indoor temperature T_i, given by expression (47), is plotted against the wall absorptance α for a summer test case when considering a solar protection glazing. Different parametric curves are shown for the ratio $S_2/S_1 = 1, 5, 7, 9, 11$. In the same plot steady simulations performed by IDA ICE were depicted by color circles. There is a perfect match between simulations and values given by expression (47) for the model parameters used in Fig. (9). In Fig. (10) the same representation is shown for a solar gain glazing which shows a higher indoor temperature (Fig.9) for the same wall absorptance α and the same ratio S_2/S_1. The reason is twofold: *(i)* beam and diffuse solar transmittance (τ, τ_d) are higher for the solar gain glazing than for the solar protection glazing and *(ii)* the absorptance of the inner glass pane is also higher (Tables 1–2).

The behavior of the winter test case is presented in Fig. 11–12. As it is observed in summer test case, the wall absorptance is not relevant in determining the indoor temperature from α =0.2 to α =1 when $S_2 > 5S_1$. When considering an almost white box ($\alpha << 1$) with a wall surface much greater than the glazing surface ($S_2 >> S_1$), the transmitted beam or diffuse radiation is reflected diffusely into the walls numerous times until is eventually absorbed. Furthermore, if $S_2 >> S_1$ the transmitted energy is absorbed regardless of the wall absorptance.

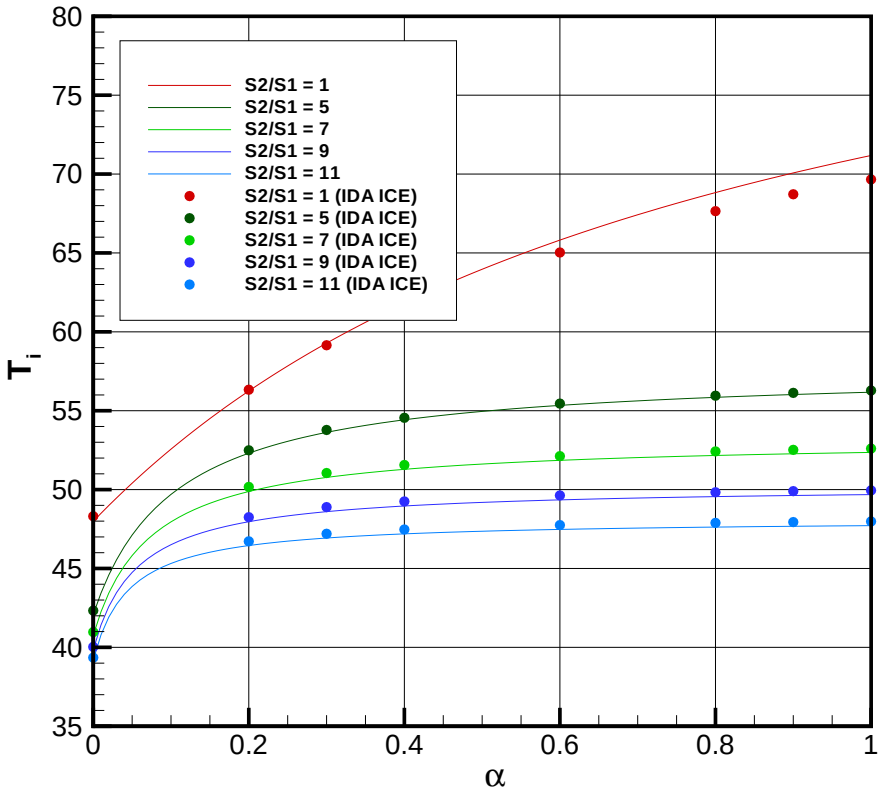

Figure 9: Steady indoor temperature T_i for the solar protection glazing versus the absorption of the walls α. The graph shows parametric curves for different surface ratios between wall surface S_2 and glazing surface S_1. Summer conditions: outdoor temperature $T_e = 35$ ^{o}C, beam solar radiation $I_b = 200$ Wm^{-2} and diffuse solar radiation $I_d = 0$.

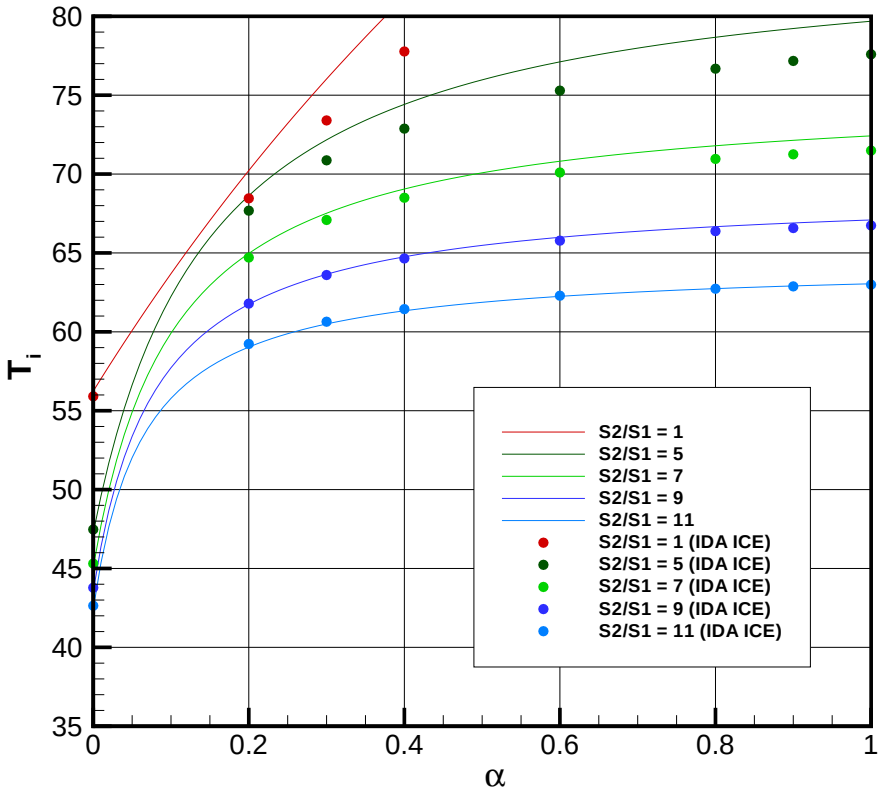

Figure 10: Steady indoor temperature T_i for the solar gain glazing versus the absorption of the walls α. The graph shows parametric curves for different surface ratios between wall surface S_2 and glazing surface S_1. Summer conditions: outdoor temperature $T_e = 35$ ^{o}C, beam solar radiation $I_b = 200$ Wm^{-2} and diffuse solar radiation $I_d = 0$.

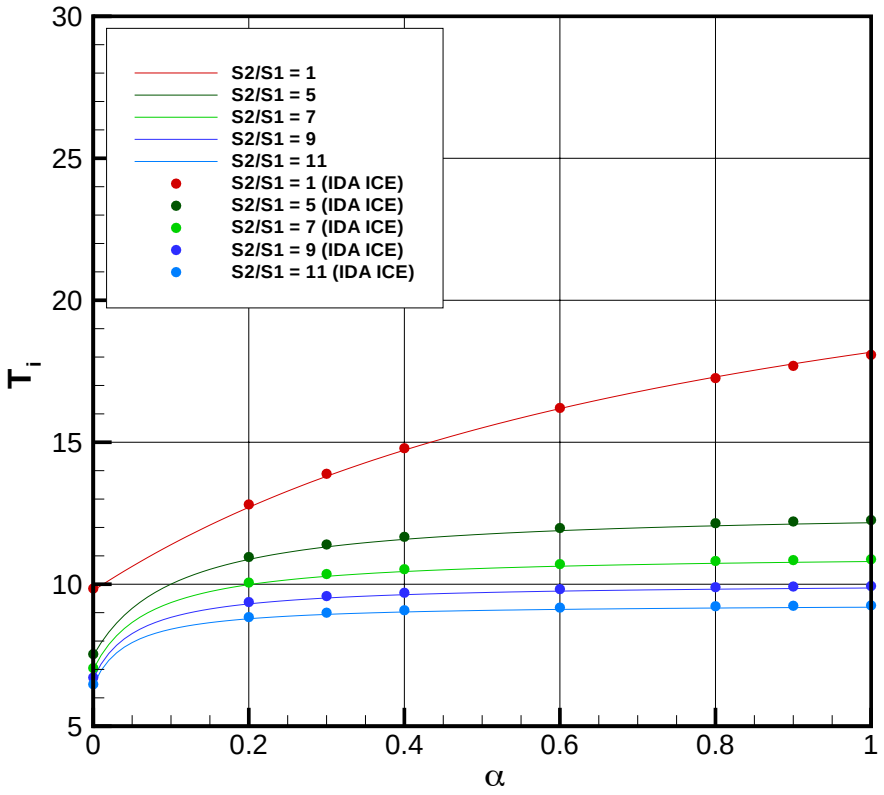

Figure 11: Steady indoor temperature T_i for the solar protection glazing versus the absorption of the walls α. The graph shows parametric curves for different surface ratios between wall surface S_2 and glazing surface S_1. Summer conditions: outdoor temperature $T_e = 5\ ^oC$, beam solar radiation $I_b = 0$ and diffuse solar radiation $I_d = 75\ \mathrm{Wm}^{-2}$.

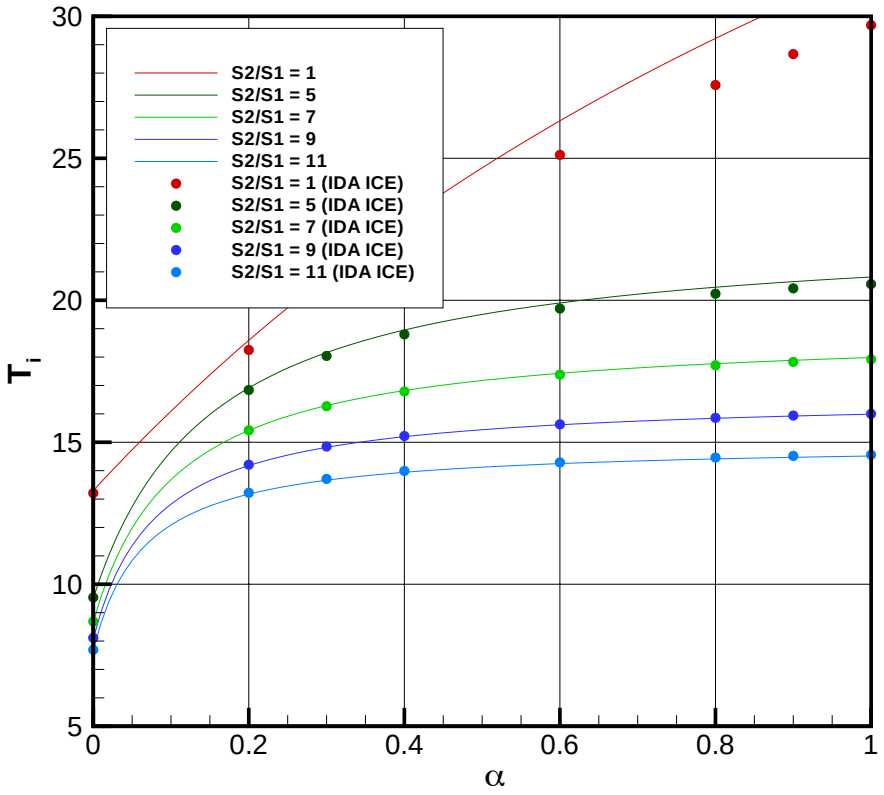

Figure 12: Steady indoor temperature T_i for the solar gain glazing versus the absorption of the walls α. The graph shows parametric curves for different surface ratios between wall surface S_2 and glazing surface S_1. Summer conditions: outdoor temperature $T_e = 5$ ^{o}C, beam solar radiation $I_b = 0$ and diffuse solar radiation $I_d = 75$ Wm^{-2}.

8. Conclusions

The election of a specific glazing determines the total absorptance of the transmitted solar energy and, consequently, the indoor room temperature. An analytical solution for the indoor temperature of rectangular rooms was obtained. This analytical solution was validated by means of complete numerical simulations carried out by the commercial software IDA ICE. The spectral problem of the solar energy distribution inside the room was initially solved. This solution allows to gauge the absorbed energy into the glass panes of the glazing and into the inner walls after multiple diffuse reflections. Once this solar energy distribution is obtained, energy balance for the glass panes and for the room allows to determine an analytical expression for the indoor temperature. This analytical solution allows to understand the relevant parameters to determine the indoor temperature. A preliminary design based on the structure of this solution allows to take decisions to set upper and lower bounds for the passive solar heating of rooms.

To summarize this analysis, the following conclusions can be derived:

1. The transmitted solar energy which is absorbed by the insulated wall is not just given by its absorptance α. The absorbed energy is increased by continuous diffuse reflections on inner surfaces and is given by the effective absorptance $\alpha_e > \alpha$.
2. The transmitted solar energy is reflected diffusely inside the room creating an irradiance. The inner walls absorb some part of the transmitted beam radiation and some part of the diffuse irradiance. The glass panes absorb beam and diffuse solar radiation together with diffuse irradiance created inside the room after multiple reflections. This absorbed energy contributes to increasing the indoor temperature.
3. There are two limit cases depending on the absorptance of inner walls: (*i*) black walls ($\alpha = 1$) and (*ii*) white walls ($\alpha = 0$). Depending on the spectral characteristics of the glazing, there are not significant differences between this two limit cases because large amount of energy can be absorbed in the glass panes when considering a white room.
4. The effective absorptance α_e of a room depends on the ratio of glazing surface to inner walls (S_1/S_2), the absorptance of inner walls and the back diffuse reflectance of the glazing (R'_d). When the inner surface S_2 is much greater than the glazing surface S_1, the effective absorptance is the unity and the absorbed energy reaches its maximum. This is due to the more efficient mechanism associated to the greater number of multiple reflections inside the room. On the contrary, if $S_2 = S_1$, some part of this energy is lost, every time the diffuse inner irradiance is reflected off the glazing.
5. The g factor has two contributions: *(i)* the secondary internal heat transfer factor A_I which is the beam and diffuse proportion of the energy which is absorbed into the glazing and later radiated indoors and *(i)* the solar transmittance τ of the glazing. The proportion of this incoming energy that is absorbed and later radiated indoors is given by the total absorptance α_t. This proportion is greater than the effective absorptance α_e due to the absorptance of inner irradiance of glass panes.

Acknowledgements

The authors would like to thank Dr. Zamecnik, Mr. Howie and Mr. Barrios for insightful discussions. This work was supported by program Horizon 2020-EU.3.3.1.: Reducing energy consumption and carbon footprint by smart and sustainable use, project ref. 680441 InDeWaG: Industrialized Development of Water Flow Glazing Systems.

References

Aguilar, J., Xamán, J., Olazo-Gómez, Y., Hernández-López, I., Becerra, G., Jaramillo, O., 2017. Thermal performance of a room with a double glazing window using glazing available in mexican market. Applied Thermal Engineering 119, 505–515.

Aste, N., Buzzetti, M., Pero, C.D., Leonforte, F., 2018. Glazing's techno-economic performance: a comparison of window features in office buildings in different climates. Energy and Buildings 159, 123–135.

Augenbroe, G., 2002. Trends in building simulation. Building and Environment 37, 891–902.

Baehr, H.D., Stephan, K., 2006. Heat and Mass Transfer. 2nd ed., Springer.

Baniassadi, A., Sailor, D.J., 2018. Synergies and trade-offs between energy efficiency and resiliency to extreme heat – a case study. Building and Environment 132, 263–272.

Bastien, D., Athienitis, A., 2000. Analysis of the solar radiation distribution and passive thermal response of an attached solarium/greenhouse. Energy Conversion and Management 41, 1247–1264.

Berardi, U., Wang, T., 2014. Daylighting in an atrium-type high performance house. Building and Environment 76, 92–104.

Causone, F., Corgnati, S.P., Filippi, M., Olesen, B.W., 2010. Solar radiation and cooling load calculation for radiant systems: Definition and evaluation of the direct solar load. Energy and Buildings 42, 305–314.

Chatziangelidis, K., Bouris, D., 2009. Calculation of the distribution of incoming solar radiation in enclosures. Applied Thermal Engineering 29, 1096–1105.

Cucumo, M., Kaliakatsos, D., Marinelli, V., 1995. Estimating effective solar absorptance in rooms. Energy and Buildings 23, 117–120.

Directive 2010/31/EU, E.P.C., 2010. Directive 2010/31/eu on the energy performance of buildings. Official Journal of the European Union, 18 June 2010 , 23.

DOE, 2010. Energyplus engineering reference. The Reference to EnergyPlus Calculations .

Dogrusoy, I.T., Tureyen, M., 2007. A field study on determination of preferences for windows in office environments. Building and Environment 42, 3660–3668.

Duffie, J.A., Beckman, W.A., 2013. Solar Engineering of Thermal Processes. 4th ed., John Wiley and Sons, Inc.

EN 410, 2011. Glass in building. Determination of luminous and solar characteristics of glazing.

EN 673, 2011. Glass in building. Determination of thermal transmittance (U value). Calculation method.

EQUA, 2017. Simulation Software URL: https://www.equa.se/.

Ferrante, G.M.A., 2000. Energy conservation and potential of a sunspace: sensitivity analysis. Energy Conversion and Management 41, 1247–1264.

Fletcher, M., Johnston, D., Glew, D., Parker, J., 2017. An empirical evaluation of temporal overheating in an assisted living passivhaus dwelling in the uk. Building and Environment 121, 106–118.

Garnier, C., Muneer, T., McCauley, L., 2015. Super insulated aerogel windows: impact on daylighting and thermal performance. Building and Environment , S0360132315300901–.

Gupta, R., Tiwari, G., 2005. Modeling of energy distribution inside greenhouse using concept of solar fraction with and without reflecting surface on north wall. Building and Environment 40, 63–71.

Hamdy, M., Carlucci, S., Hoes, P.J., Hensen, J.L., 2017. The impact of climate change on the overheating risk in dwellings—a dutch case study. Building and Environment , S0360132317302664–.

Hee, W., Alghoul, M., Bakhtyar, B., Elayeb, O., Shameri, M., Alrubaih, M., Sopian, K., 2015. The role of window glazing on daylighting and energy saving in buildings. Renewable and Sustainable Energy Reviews 42, 323–343.

Huang, Y., lei Niu, J., 2016. Optimal building envelope design based on simulated performance: History, current status and new potentials. Energy and Buildings 117, 387–398.

Inanici, M.N., Demirbilek, F., 2000. Thermal performance optimization of building aspect ratio and south window size in five cities having different climatic characteristics of turkey. Building and Environment 35, 41–52.

Jenkins, D., Peacock, A., Banfill, P., 2009. Will future low-carbon schools in the uk have an overheating problem? Building and Environment 44, 490–501.

Kazanasmaz, T., Grobe, L.O., Bauer, C., Krehel, M., Wittkopf, S., 2016. Three approaches to optimize optical properties and size of a south-facing window for spatial daylight autonomy. Building and Environment 102, 243–256.

Kim, G., Kim, J.T., 2010a. Healthy-daylighting design for the living environment in apartments in korea. Building and Environment 45, 287–294.

Kim, J.T., Kim, G., 2010b. Overview and new developments in optical daylighting systems for building a healthy indoor environment. Building and Environment 45, 256–269.

Konroyd-Bolden, E., Liao, Z., 2015. Thermal window insulation. Energy and Buildings 109, 245–254.

Kontoleon, K., 2012. Dynamic thermal circuit modelling with distribution of internal solar radiation on varying façade orientations. Energy and Buildings 47, 139–150.

Kontoleon, K., 2015. Glazing solar heat gain analysis and optimization at varying orientations and placements in aspect of distributed radiation at the interior surfaces. Applied Energy 144, 152–164.

Kumar, G.K., Saboor, S., Babu, T.A., 2017. Experimental and theoretical studies of window glazing materials of green energy building in indian climatic zones. Energy Procedia 109, 306–313.

Kyoto Protocol, U.N., 2005. Kyoto protocol. United Nations Framework Convention on Climate Change, Kyoto 11 December 1997 .

Lai, C.M., Hokoi, S., 2015. Solar façades: A review. Building and Environment 91, 152–165.

Lu, S., Li, Z., Zhao, Q., Jiang, F., 2017. Modified calculation of solar heat gain coefficient in glazing façade buildings. Energy Procedia 122, 151–156.

Lyons, P., Wong, J., Bhandari, M., 2010. A comparison of window modeling methods in energyplus 4.0. Fourth National Conference of IBPSA-USA .

Modest, M.F., 1982. A general model for the calculation of daylighting in interior spaces. Energy and Buildings 5, 69–79.

Mottard, J.M., Fissore, A., 2007. Thermal simulation of an attached sunspace and its experimental validation. Solar Energy 81, 305–315.

Oliveti, G., Arcuri, N., Bruno, R., Simone, M.D., 2011. An accurate calculation model of solar heat gain through glazed surfaces. Energy and Buildings 43, 269–274.

Paris Agreement, U.N., 2016. Paris agreement. United Nations Framework Convention on Climate Change, Paris 5 October 2016 .

Romero, X., Hernández, J.A., 2017. Spectral problem for water flow glazings. Energy and Buildings 145, 67–78.

Sameni, S.M.T., Gaterell, M., Montazami, A., Ahmed, A., 2015. Overheating investigation in uk social housing flats built to the passivhaus standard. Building and Environment 92, 222–235.

Sierra, P., Hernández, J.A., 2017. Solar heat gain coefficient of water flow glazings. Energy and Buildings 139, 133 – 145. doi:http://dx.doi.org/10.1016/j.enbuild.2017.01.032.

Sparrow, E., Cess, R., 1978. Radiation Heat Transfer. Reprint edition ed., CRC Press.

Ulpiani, G., Benedettelli, M., di Perna, C., Naticchia, B., 2017. Overheating phenomena induced by fully-glazed facades: Investigation of a sick building in italy and assessment of the benefits achieved via model predictive control of the ac system. Solar Energy 157, 830–852.

Wall, M., 1995. A design tool for glazed spaces: Part I description. ASHRAE Transactions 101, 1261–1271.

Wall, M., 1997. Distribution of solar radiation in glazed spaces and adjacent buildings: A comparison of simulation programs. Energy and Buildings 26, 129–135.

Wen, J., Smith, T.F., 2002. Absorption of solar energy in a room. Solar Energy 72, 283–297.

Xamán, J., Olazo-Gómez, Y., Chávez, Y., Hinojosa, J., Hernández-Pérez, I., Hernández-López, I., Zavala-Guillén, I., 2016. Computational fluid dynamics for thermal evaluation of a room with a double glazing window with a solar control film. Renewable Energy 94, 237–250.

Yao, J., Zhu, N., 2012. Evaluation of indoor thermal environmental, energy and daylighting performance of thermotropic windows. Building and Environment 49, 283–290.